Second International Conference on CFD in the Minerals and Process Industries
CSIRO, Melbourne, Australia
6-8 December 1999

CFD MODELLING OF A STIRRED BEAD MILL FOR FINE GRINDING

Graeme L. LANE

CSIRO Minerals, Box 312, Clayton Sth, Victoria 3169 AUSTRALIA

ABSTRACT

Stirred bead mills find application in a number of industries where there is a need for very fine grinding or particle dispersion. In the minerals industry this type of mill is becoming increasingly important due to processing of ore bodies which are fine-grained and require milling to fine sizes for effective mineral liberation. Numerical simulation of these mills offers a means of understanding the motion of particles and fluid in the mill, which should assist in process development and optimisation. CFD modelling has been developed for a laboratory-scale Netzsch horizontal bead mill. The details of the internal geometry including the rotor with attached discs are modelled using a multi-block body-fitted finite volume method. The mixture of grinding beads, fine product particles and water are treated as a single fluid, and the equations of conservation of mass and momentum are solved numerically in a rotating frame of reference. Simulation results indicate that the flow pattern consists of a series of distinct mixing cells between the rotor discs. It appears that material is drawn through the holes and redistributed between compartments, thus enhancing axial dispersion. Local energy dissipation is non-uniform with most energy dissipation occurring in a small fraction of the volume, and most of the grinding is expected to take place within these zones, so that effective grinding may depend on circulation of all particles through these zones. Due to backmixing in the mill, product exiting the mill exhibits a wide residence time distribution. The residence time distribution was obtained by simulation and is compared with experimental measurements.

Keywords: Stirred bead mill, stirred media mill, CFD, fine grinding, residence time distribution.

NOMENCLATURE

C	concentration of tracer (-)
$\mathcal{D}$	diffusivity (m^2s^{-1})
E	exit age distribution function (s^{-1})
g	acceleration due to gravity (ms^{-2})
P	energy dissipation rate (W m^{-3})
S	shear rate (s^{-1})
t	time
U	velocity (m s^{-1})
v	velocity (m s^{-1})
Φ_v	viscous energy dissipation function (s^{-2})
μ	effective viscosity (Pa.s)
ρ	density (kg/m^3)

INTRODUCTION

Stirred bead mills, also known as stirred media mills, find application in a number of industries, where they are used for fine grinding of particulates or fine dispersion of agglomerates [1]. In the minerals industries, fine grinding in stirred mills is becoming increasingly important, since available ore bodies are increasingly fine-grained and require milling to fine sizes for effective mineral liberation. Numerical modelling of the particle and fluid motion in these mills offers a means of obtaining further understanding, which should assist in process development, scale-up and optimisation. This paper describes progress in developing CFD modelling for a Netzsch horizontal bead mill. This mill was chosen because it follows a commonly-used design, and in addition some experimental data has been obtained for this mill which may be used for comparison with CFD predictions.

BACKGROUND

Stirred bead mills consist basically of an enclosed water-jacketed cylindrical vessel fitted with an agitator and filled to about 80% of the close-packing limit with grinding media, which are normally steel or ceramic beads ranging 1 – 5 mm in diameter. The remaining volume is filled with a suspension (slurry) of the material to be ground. Typical feed size is less than 100 microns and product size is usually 1 to 10 micron. Many designs of stirred mills are available [1], which may be classified broadly according to the orientation as horizontal or vertical bead mills. The stirrer usually consists of a shaft fitted with either discs or pins, and in addition there may be stator pins.

Previous literature [1-3] describes the main principles of fine grinding in stirred bead mills. The grinding mechanism occurs due to fine particles being trapped and stressed between moving beads which are accelerated by the agitator and collide or rub against each other. The efficiency and the grinding rate depend on several variables such as the agitator speed and the size of the grinding beads. A suspension of the material to be ground is pumped through the mill continuously, while at the outlet end of the mill, the beads are retained by some separation device. Due to the net movement of suspension along the length of the mill, the beads tend also to move towards the outlet. Therefore, the mill must allow some degree of backmixing so as redistribute the beads through the mill. However, a consequence of this is that the slurry is also back-mixed, and the product leaving the mill has a wide residence time distribution characteristic of axial

dispersion. Due to unequal grinding times, a wide product size distribution may result. The flowrate of suspension through the mill is also limited because as the flowrate is increased, the backmixing of the beads becomes ineffective and hydraulic packing develops, where the beads migrate to the outlet end and become packed. For effective operation of bead mills these limitations must be taken into account.

By modelling the bead mill, it is hoped to capture some of these features of operation. This may lead to better understanding of the mechanisms in bead mills and provide a tool which can assist in development and optimisation.

In a previous computational study [4], the axisymmetric flow around a single solid disc in a horizontal mill was simulated. Results indicated that in addition to rotational motion, there is a series of circulatory cells in the axial - radial plane through the mill, where the material close to each disc is accelerated radially outwards to the wall and returns to the shaft in the space between the discs. It was found also that about 80-90% of the energy dissipation occurs in 10-20% of the mill volume. The present simulation work confirms these findings.

DETAILS OF THE MILL

The model was developed for a Netzsch horizontal stirred mill 122 mm internal diameter, 392 mm in length, and with a volume of about 4 litres. The rotor consists of a shaft 35 mm diameter fitted with nine discs, each 12.6 mm thick, 100 mm diameter and spaced 29 mm apart. Each of the discs has five holes through it, spaced on a circle of radius 32 mm. The grinding chamber is filled to approximately 80% of the close-packing limit with spherical grinding media about 1 - 2 mm diameter. The remaining volume is filled with a suspension of fine solids, which is pumped through the chamber entering at one end and exiting at the other end, where the rotor drive is mounted. The outlet is in the form of a "dynamic gap", which is a 0.25 mm gap between the rotating shaft and the stationary end of the mill casing. This serves as a self-cleaning sieve mechanism, which prevents the coarse grinding balls from exiting the mill.

Operating conditions for the CFD simulations were chosen to correspond to conditions for which experimental residence time distribution (RTD) data has been obtained. The material being ground in these experiments was a slurry of zinc ore concentrate, about 25% v/v solids (60% w/w) and 80% passing 27 μm at the inlet, with a feed rate of 1.5 l/min. Grinding beads were zircon, about 50% v/v. Rotor speed was 1500 rpm.

METHOD

Interpretation of particle and fluid mechanics

The beads, ore particles and water are three distinct components which could each potentially be considered as a separate phase in the modelling. However, given the fineness of the ore particles, these particles may be expected to follow the liquid streamlines closely and one may assume that, in terms of the bulk flow, water and ore particles behave a single slurry phase. The grinding beads are much larger and in general would not be expected to follow the streamlines of the surrounding fluid due to inertia and gravity effects. However, the beads are highly constrained, being present at 80% of their packed volume limit, which implies that the average spacing between beads is only a small percentage of the bead diameter and in fact there is very little scope for variations in bead concentration. Although extreme conditions may occur where the beads are fully packed together ("hydraulic packing"), the present study is limited to conditions where the beads remain mixed with slurry, and thus the beads and slurry may be regarded as a homogeneous single phase, at least from a *macroscopic* point of view. Thus a single phase is modelled using appropriate effective properties. Density of this fluid is readily calculated by weighting the density of the components. Describing the viscosity of the mixture is more problematic. A large contribution to the effective viscosity would be expected to come from the inelastic collisions between grinding beads. A relatively high value of viscosity can be expected for the mixture, but the viscosity is not necessarily Newtonian. However, from the work of Blecher et al. [4] a constant value of about 1.0 Pa s can be inferred, and this value is also adopted here, although different values for viscosity or models for non-Newtonian viscosity can be readily incorporated in the CFD model.

Although the mixture is taken as homogeneous for the purpose of calculating the mean flow, there is of course relative motion between components on a *microscopic* level, where beads collide with each other, trapping and stressing the smaller ore particles at the same time, leading to breakage. Thus, the grinding rate may be expected to relate to the frequency and energy of collisions between beads. It is therefore likely, as a first approximation, that an indication of the local intensity of grinding may be obtained from the viscous energy dissipation rate, P, which can be calculated as a function of viscosity and mean velocity gradients according to:

$$P = \mu \Phi_v , \tag{1}$$

where μ is the viscosity and Φ_v is the energy dissipation function calculated as [5]:

$$\Phi_v = 2\left[\left(\frac{\partial v_x}{\partial x}\right)^2 + \left(\frac{\partial v_y}{\partial y}\right)^2 + \left(\frac{\partial v_z}{\partial z}\right)^2\right] + \left(\frac{\partial v_y}{\partial x} + \frac{\partial v_x}{\partial y}\right)^2 + \left(\frac{\partial v_z}{\partial y} + \frac{\partial v_y}{\partial z}\right)^2 + \left(\frac{\partial v_x}{\partial z} + \frac{\partial v_z}{\partial x}\right)^2 \tag{2}$$

The local shear rate may be used equivalently, where shear rate is defined in terms of the energy dissipation function according to:

$$S = \sqrt{\Phi_v} . \tag{3}$$

CFD Modelling

A number of CFD simulations have been carried out adopting several alternative approaches to simulating the flow in the horizontal stirred mill. The various methods are described below. In each case the geometry is specified using a multi-block body-fitted finite volume mesh, and a numerical solution for the velocity field is obtained using the commercial software CFX4.2. The fluid flow is specified by the equations for conservation of mass and

momentum of an incompressible fluid, which may be given as:

$$\nabla \bullet \vec{U} = 0 \quad (4)$$

$$\nabla \bullet (\rho \vec{U} \otimes \vec{U}) = -\nabla P + \nabla \bullet (\mu(\nabla \vec{U} + (\nabla \vec{U})^T)) + \rho \vec{g} \quad (5)$$

Method 1

In the first instance a model was set up to represent the entire mill interior as close as possible to the manufacturer's specifications, including the rotor shaft with nine discs each with five holes (Figure 1). To account for rotation of the rotor, a sliding grid method was used, where the equations are solved in time-dependent form, and at each time step the section of the grid containing the rotor is rotated by an incremental angle. The number of cells was limited to about 150 000 in order to achieve practical computational times, however due to the complex geometry, resolution of the flow field was fairly poor. However, sufficient detail was obtained by these preliminary results to provide insight into the flow pattern, which has allowed the development of more efficient simulation methods using reasonable simplifications of the geometry.

Method 2

The results using method 1 indicate a flow pattern consisting of distinct axial-radial circulation cells in zones between each disc and the centreline between discs. Furthermore, in the azimuthal direction it is likely that the same flow pattern is repeated around each of the five holes in each disc. Thus, to study the flow in more detail, a small section of the mill was modelled, which neglecting end effects may be regarded as the basic repeating unit in the mill. This section consists of a 72° section surrounding a single hole in a single disc, and extending axially to planes half way between the disc and neighbouring discs. The grid for this simplified geometry is shown in Figure 2, and was constructed using a multi-block grid with 6 blocks and 16 500 cells. Periodic boundaries are applied in the azimuthal direction, while the end planes in the axial direction are taken to be symmetry planes. Further computational efficiency was achieved by using a rotating frame of reference, where the rotor appears stationary and the wall is assigned an angular velocity equal in magnitude and opposite in sign to the rotor. The equations were solved in steady-state form with satisfactory convergence in 1500 iterations.

Method 3

Having established the basic flow pattern in the assumed repeating unit of the flow, a further simulation was carried out again applying periodic boundaries in the azimuthal direction to a 72° section, but now modelling the entire length of the mill. In this case the grid consisted of 55 blocks and 111 900 cells. Due to the assumed periodicity in the tangential direction, much better grid resolution is possible compared to modelling the whole of the mill as in Method 1.

A steady-state approach to the solution was attempted with this method, however satisfactory convergence could not be achieved. Therefore, the flow field prediction was obtained using explicit time-stepping, stopping the calculation after 400 time steps of 0.04 seconds with 20 iterations per time step. Although convergence was obtained for each time step and a fully developed and characteristic flow pattern was obtained, no steady solution was ever obtained. By comparison, the simulation of the single disc appears to converge readily because of the artificial constraint of symmetry planes between discs. Without this constraint, the circulation loops in the flow appear to wander around and vary with time, and it is possible that there is no steady solution to the equations of motion.

Method 4

The CFD modelling has been extended to calculate the residence time distribution (RTD) of ore particles in the mill. Similar to the typical experimental approach, this is obtained by measuring the response at the outlet to a change in concentration, C, of a tracer at the inlet of the apparatus. The transport equation for the tracer concentration is:

$$\frac{\partial C}{\partial t} + \nabla \bullet (\vec{U} C - \mathcal{D} \nabla C) = 0 . \quad (6)$$

Simulation of the tracer response requires a time-dependent approach where the calculation should be advanced in small time steps, certainly no larger than the period of rotation of the stirrer. A time step of about 0.02 seconds was adopted, but on the other hand the nominal slurry residence time is 80 seconds (based on plug flow), so that a very large number of time steps is required. To achieve reasonable computation times, further simplification of the geometry was necessary. In this case, an axisymmetric model was assumed in a radial-axial plane with a total of about 19 200 cells. The justification for this assumption is that the tracer should mix quickly in the azimuthal direction, whereas it is the movement of tracer in the axial direction which is of interest. In this model, the holes were assigned an effective area porosity corresponding to the fraction of area occupied by the holes. Using this geometry, a steady solution for the velocity field was first obtained, which was then used for the time-dependent solution of the scalar equation. Concentration was logged at the outlet in reponse to a step change at the inlet. From the response, $C(t)$, the exit age distribution $E(t)$ (or residence time distribution) may be calculated according to [6]:

$$E(t) = \frac{dC}{dt} \quad (7)$$

The diffusivity $\mathcal{D}$ in equation (6) may be expected to be orders of magnitude higher than a typical molecular diffusivity, due to a mechanism of dispersion in which material is "squeezed out" in random directions during collisions between the grinding beads. However, no measured value for the diffusivity was available, so a value was estimated as a fitted parameter to try to match the experimental data.

RESULTS AND DISCUSSION

Various approaches are described above which were taken in modelling the flow in the Netzsch horizontal bead mill. The number of different approaches has resulted because of the need to obtain results within a reasonable period of time given the constraints of available computer resources. In Method 1 where the whole of the mill was modelled, reasonable computational time was only achieved for a

low resolution grid. Therefore, to improve computational efficiency, simplifications to the model geometry were proposed. Despite fairly low resolution of the flow field using Method 1, the results indicated that the flow pattern consists of a number of distinct axial-radial recirculation cells, two between each disc. Furthermore, it appeared that the flow pattern adjacent to each hole on a disc should be similar. Therefore, in Method 2 the flow was calculated for a small 72° section of the mill surrounding one hole on one disc, which may be regarded as the basic repeating unit in the mill.

Figure 3 shows the velocity vectors in a radial-axial plane through the centre of the mill, parallel to the axis, as obtained by Method 2, where periodicity of a 72° section was assumed and just a single disc was modelled. Figure 4 shows the velocity vectors in a perpendicular plane, half way between a disc and the assumed plane of symmetry. Figure 6 shows the equivalent results in a radial-axial plane when modelling the full length of the mill as in Method 3. In both simulations it is found that the material in the mill has a complex spiralling pattern, where as well as moving in an azimuthal motion in the direction of agitator rotation, there is a series of circulatory mixing cells in the radial-axial plane, where the shearing action of each disc causes the mixture to be centrifuged radially outwards towards the outer wall. The fluid then impinges on the outer wall and and is drawn radially inwards again. There are some differences in the two simulations. In modelling a single disc, a symmetrical pattern is obtained with one circulation cell on each side of the disc (Figure 3). However, this symmetry appears to result from the artificial assumption that the mid-planes between discs are symmetry planes. In Method 3 this assumption does not apply, and Figure 6 shows that symmetry is not maintained, and instead the circulation loops vary in size and position. Again, there are generally two circulation loops per compartment between discs, but there are also smaller circulation loops in the gap between the disc edge and outer wall.

The distribution of shear rates in a radial-axial plane is shown in Figure 5, based on Method 2. High shear rates are generated due to the relative movement between discs and the outer wall. The highest shear rates correspond to the highest local rates of energy dissipation, and it is found that most of the energy dissipation occurs in a small volume surrounding the outer part of the discs and at the outer wall. This finding agrees with the previous study of Blecher et al. [4]. Most of the grinding would be expected to take place in these zones. Thus, grinding of all particles may depend on the circulation of particles in and out of these zones of high energy dissipation.

The velocity patterns (Figures 3 and 6) indicate that the mixture of suspension and beads is drawn into a hole at the lower radius side and then ejected back into the bulk of the fluid from the outer (high radius) part of the hole. This fluid motion corresponds to a pressure gradient within the hole (not shown here). It would appear that material which reaches the centreline of the hole may subsequently exit to either side, and the effect of this is that material is redistributed along the length of the mill, leading to back-mixing in the mill. This effect is apparently intended [5] and is aimed at preventing a build-up of grinding beads at the slurry outlet. Since fine particles are also redistributed by flow through the holes, this leads to a wider residence time distribution.

Results of CFD simulation of the RTD are shown in Figure 7 along with experimental tracer results. Qualitatively, both methods give a similar curve with a very broad RTD, which indicates axial dispersion of slurry particles. Both curves indicate early exiting, with the peak in the distribution occurring considerably earlier than the nominal mean residence time of 80 seconds (calculated based on plug flow), and the curves also show long tail. However, the peak in the CFD result occurs at a time only about half of that in the experimental result.

The prediction of the RTD depends on modelling of both convective and diffusive processes (see equation (6)). In another run, the diffusion coefficient was set to be several orders of magnitude lower, and it was found that the tracer species essentially remained in the first two mixing cells and did not spread to the outlet at all. Therefore, diffusion is necessary to move the tracer between successive mixing cells in the mill, and the resulting prediction of RTD is therefore sensitive to the choice of diffusion coefficient. However, the diffusion coefficient was only roughly estimated, and the prediction of the RTD could therefore be improved by a more accurate value for the diffusion coefficient. In addition, the convective term in the scalar transport equation depends on an accurate estimate of the velocity field, and further improvement may also be necessary in this respect. For greater confidence in the velocity predictions, a better estimate of the mixture viscosity would be required. Experimental data for the fine particle diffusion coefficient and the mixture viscosity may be needed.

In summary, the present CFD study has shown that a range of information may be obtained by modelling stirred bead mills including velocities, shear rates and residence time distributions. Further refinement of the modelling method may be expected to improve the accuracy of results. It is suggested that CFD may provide a useful alternative to experimental studies, which may be very difficult or time consuming, and in addition the CFD method may be applied readily to full-scale equipment. It is expected that the method could be readily applied to other mill designs besides the Netzsch mill studied here. Hence, there is the potential to use the CFD method for investigating and comparing different mill geometries or different operating conditions. Also, it would be possible using the CFD method to track the paths of particles through the mill, integrating the time spent at different levels of shear in the mill. This could provide a starting point for developing a model of grinding in the mill.

CONCLUSIONS

CFD modelling of a horizontal stirred mill has provided predictions of the flow pattern, velocities and distribution of shear rates with the mill. The results reveal a flow pattern in which material circulates in a series of mixed zones around the discs. Most of the energy dissipation is found to occur in a small fraction of the total internal volume close to the disc surface and at the wall, so that the grinding of all particles may depend on their recirculation to these high energy zones. The predicted flow pattern suggests that the mixture of beads and slurry is drawn

through the holes, which promotes back-mixing of the grinding beads.

By simplifying the model to an axisymmetric model in an axial-radial plane, the flow of a tracer species from inlet to outlet was simulated to obtain a residence time distribution. The predicted RTD curve has a similar shape to the experimental measurements although the peak in the distribution is earlier in the CFD result. It is anticipated that improved agreement will result by obtaining experimental data for diffusivity and viscosity. The modelling method has the potential to be applied to other mill designs, and could be used for comparing alternative geometries and investigating the distribution of energy dissipation. The CFD method might also provide a basis for modelling of grinding in the mill.

ACKNOWLEDGMENT

The author wishes to acknowledge K. R. Weller, M.-W. Gao and Y. Liu at CSIRO Minerals for providing the experimental data for residence time distribution in the horizontal bead mill.

REFERENCES

1. STEHR, N., 1988, "Recent Developments in Stirred Ball Milling", *Int J Min Proc*, Vol. 22, pp. 431-444.
2. ROELOFSEN, D.P., 1991, "Developments in dispersing technology", *EuroCoat*, 3/1991, pp. 128-144.
3. BELFADHEL, H. and FRANCES, C., 1997, "Modelling fine grinding in a stirred bead mill", *Proceedings of the XX IMPC*, Aachen, 21-26 September 1997, pp. 91-100.
4. BLECHER, L., KWADE, A. and SCHWEDES, J., 1996, "Motion and stress intensity of grinding beads in a stirred media mill. Part 1: Energy density distribution and motion of single grinding beads", *Powder Technology*, Vol. 86, pp. 59-68.
5. BIRD, R.B., STEWART, W.E. and LIGHTFOOT, E.N., 1960, *Transport Phenomena*, John Wiley & Sons, p. 91.
6. LEVENSPIEL, O., 1972, *Chemical Reaction Engineering*, 2nd Edition, John Wiley & Sons, New York, p. 259.

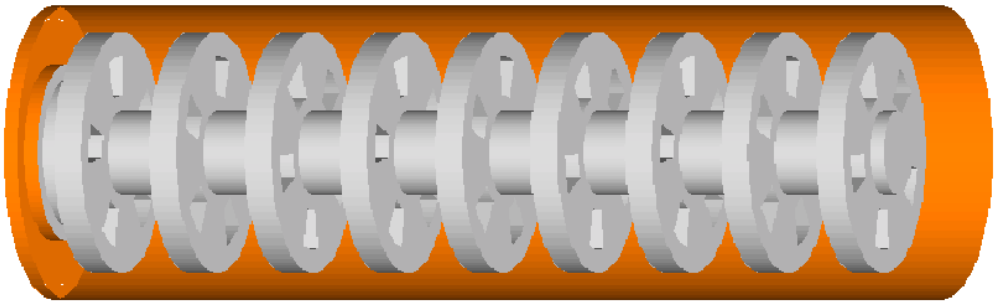

Figure 1: CFD representation of the full geometry of the Netzsch horizontal bead mill (Method 1).

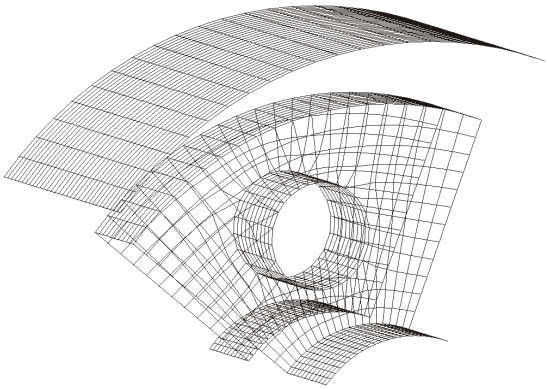

Figure 2: Finite volume grid for single disc simulation (Method 2).

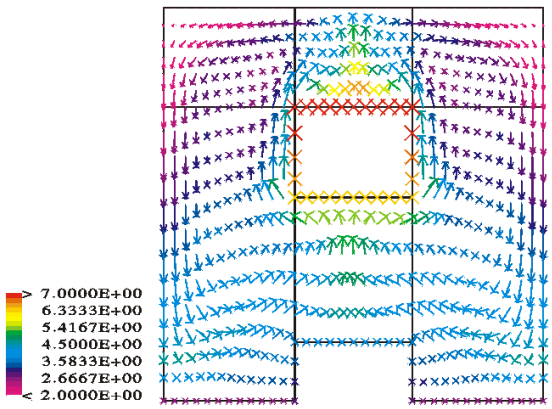

Figure 3: Velocity vectors (m/s) in a radial-axial plane centred on a hole – single disc simulation (Method 2).

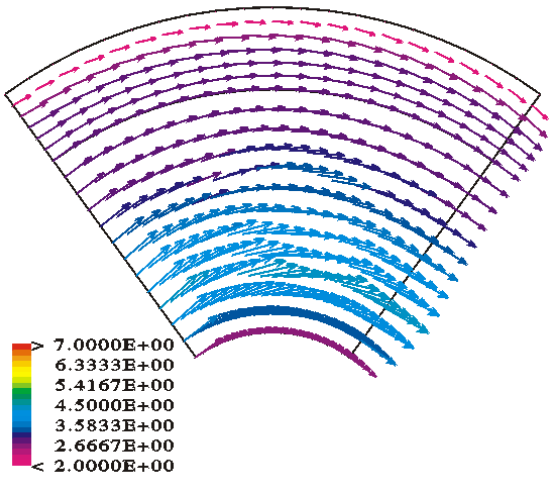

Figure 4: Velocity vectors (m/s) in a plane perpendicular to axis and half way between disc and end plane of symmetry – single disc simulation (Method 2).

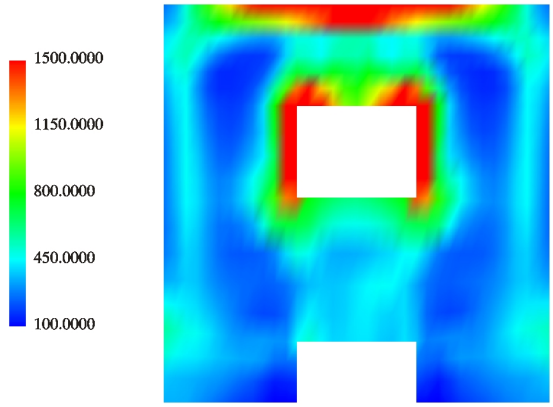

Figure 5: Shear rate distribution in radial-axial plane centred on a disc (Method 2).

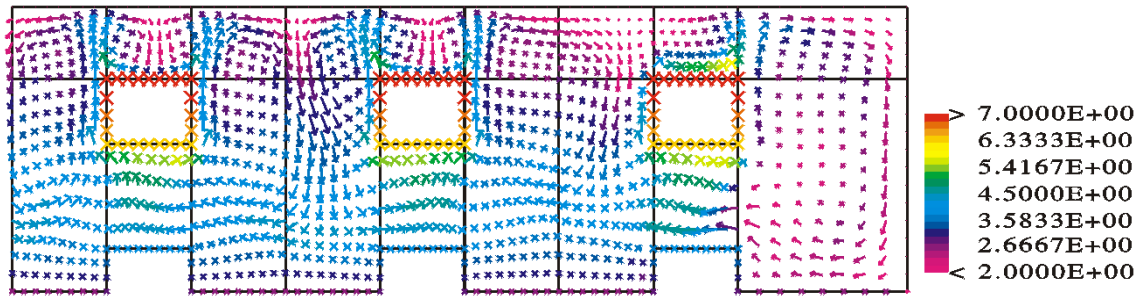

Figure 6: Velocity vectors (m/s) in a radial-axial plane centred on holes. Simulation of full length of mill (Method 3) but showing just the last three discs on shaft and end wall.

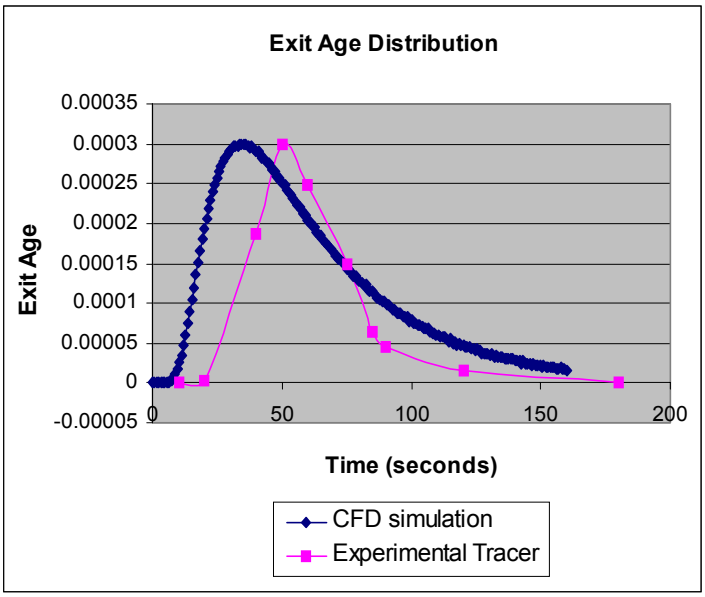

Figure 7: Residence time distribution of mill: experimental measurement and CFD prediction.